Application of Higher Order Statistics Techniques to EMG Signals to Characterize the Motor Unit Action Potential

Shahjahan Shahid*, Jacqueline Walker, *Member, IEEE*, Gerard M. Lyons, Ciaran A. Byrne, and Anand Vishwanath Nene

***Abstract*—The electromyographic (EMG) signal provides information about the performance of muscles and nerves. At any instant, the shape of the muscle signal, motor unit action potential (MUAP), is constant unless there is movement of the position of the electrode or biochemical changes in the muscle due to changes in contraction level. The rate of neuron pulses, whose exact times of occurrence are random in nature, is related to the time duration and force of a muscle contraction.**

The EMG signal can be modeled as the output signal of a filtered impulse process where the neuron firing pulses are assumed to be the input of a system whose transfer function is the motor unit action potential. Representing the neuron pulses as a point process with random times of occurrence, the higher order statistics based system reconstruction algorithm can be applied to the EMG signal to characterize the motor unit action potential.

In this paper, we report results from applying a cepstrum of bispectrum based system reconstruction algorithm to real wired-EMG (wEMG) and surface-EMG (sEMG) signals to estimate the appearance of MUAPs in the Rectus Femoris and Vastus Lateralis muscles while the muscles are at rest and in six other contraction positions. It is observed that the appearance of MUAPs estimated from any EMG (wEMG or sEMG) signal clearly shows evidence of motor unit recruitment and crosstalk, if any, due to activity in neighboring muscles. It is also found that the shape of MUAPs remains the same on loading.

***Index Terms*—Electromyographic signals, higher order statistics theory, HOS-based blind deconvolution, motor unit action potential.**

I. Introduction

ELECTROMYOGRAPHIC (EMG) signals, detected directly from the muscle or from the skin surface by using indwelling or surface electrodes, respectively, show a train of motor unit action potentials (MUAPs) plus noise. An MUAP is the sum of a group of muscle fiber action potentials (MFAP), where each MFAP is the superimposed information of the muscle and neuron firing signals [1], [2]. To maintain or increase a force level, the motor unit (alpha motoneuron) fires (excites each muscle fiber) repeatedly and, consequently, the muscle contracts. The firing pulses are normally considered a random function of time which is non-Gaussian in nature [3]. A simple model of an EMG signal is [1]–[3]

$$x(n) = \sum_{r=0}^{N-1} h(r)e(n-r) + w(n) \tag{1}$$

where $x(n)$ is the modeled EMG signal, $e(n)$ is a point process, whose times of occurrence have a random characteristic, that represents the firing impulses, $h(r)$ represents the MUAP, $w(n)$ is a zero mean additive white Gaussian noise which is independent of $e(n)$ that represents the system noise and N is the number of motor unit firings.

There are many factors which can affect the appearance of the MUAP, including the type of electrodes, e.g., whether they are invasive or noninvasive and the filtering properties of the electrode [1]. The shape and the amplitude of the MUAP may also depend on the characteristics of the muscle fibers and the distance between the muscle fiber and the recording site [1]. The amplitude of the MUAP in the EMG signal is related to a certain extent to the force a muscle may generate and thus to the level of contraction [1], [4]. The shape of the MUAP within the motor unit action potential train (MUAPT) is constant unless there is movement of the position of the electrode from where the EMG signal is recorded, or biochemical changes in the muscle occur [1]. The frequency of occurrence of the MUAP in the EMG signal also changes at different levels of muscle contraction [5].

To characterize the EMG signal, investigators have used a variety of signal processing techniques. Due to the difficulty of extracting individual MUAPs from the EMG signal, particularly the sEMG signal, many investigators have relied on the use of the overall signal. The amplitude of the EMG signal, estimated as either the mean absolute value (MAV) or root mean square (RMS) of its time-varying standard deviation, may be recovered by de-correlating the signal (following appropriate noise rejection filtering), then demodulating and smoothing it [6]. Parameters such as the RMS value have been extensively used to assess the relationship between the EMG amplitude and the force of the contraction [4], [7], [8], [13]. The integrated EMG signal may also be used: for example, a linear relationship between the

Manuscript received April 7, 2004; revised January 27, 2005. *Asterisk indicates corresponding author.*

*S. Shahid is with g.tec Guger Technologies OEG, Herberstein str. 60, 8020, Graz, Austria (e-mail: shahid@gtec.at).

J. Walker and G. M. Lyons are with the Biomedical Electronic Laboratory of the Department of Electronic and Computer Engineering, University of Limerick, Limerick, Ireland.

C. A. Byrne is with BioMedical Research Ltd., Parkmore Business Park West, Galway, Ireland.

A. V. Nene is with the Department of Physical and Rehabilitation Medicine, Roessingh Research and Development, Enschede 7500-AH, The Netherlands.

Digital Object Identifier 10.1109/TBME.2005.847525

amplitude of the raw integrated wired EMG signal and the force level in the Vastus Lateralis (VL) muscle during linear ramp isometric knee extension was found by [9]. A linear correlation was also observed in the average integrated EMG signals recorded from any place in the VL muscle. Evidence of crosstalk in the sEMG signal of the Rectus Femoris (RF) muscle due to the contraction of the Vastus Lateralis (VL) muscle was found by an ensemble averaging technique applied to both the surface EMG (sEMG) and wired EMG (wEMG) signals [10], [11].

A number of techniques have been developed to assess EMG signals (both wEMG and sEMG) in the frequency domain. The spectrum of the EMG signal is mainly composed of energy in frequencies ranging between 50 to 70 Hz [12]. The frequency spectrum may change due to physiological processes, such as fatigue [13]. The change in the frequency spectrum of the fatigued muscle EMG signal is a reduction in the power in the higher frequencies which suggests that a different type of MUAP may be generated due to the physiological processes in the muscle. A similar behavior of frequency shifting and power reduction at high frequency was observed in the sEMG signal [12]. Higher order statistics were used by [3] to analyze the sEMG signal. It was reported that the sEMG becomes less Gaussian on increasing mean voluntary contraction (MVC).

Some researchers have worked on establishing the shape of the MUAP in the EMG signal. A low-pass differentiator was described in [13] for estimating MUAPs from the EMG signal. A concentric needle electrode was used to record the EMG signal and the MUAP parameters of duration and number of baseline crossing pulses were visually assessed and measured from the recorded signal by [14]. However, it is very difficult to determine MUAPs when a great number of motor units fire simultaneously. MUAPs were extracted from the wEMG signal by searching and matching with a pattern (template) of MUAPs that had previously been observed [15], [16].

A template-based approach can work in signals from weakly contracting muscle as distinct MUAPs can be distinguished more clearly during weak contractions when only a few motor units are active. But with strong contractions, the MUAPs become so numerous that the EMG signal becomes noise-like in appearance [15]. In these circumstances, a signal processing technique may be applied to extract the MUAPs. As a first step toward this goal a weighted low pass differential filter was proposed by [17] to locate MUAPs in the sEMG by estimating their peaks in the sEMG signal. A Wiener filter based sEMG signal decomposition was proposed by [18]. The proposed method theoretically can estimate the intramuscular EMG signal, i.e., the MUAP when the firing pulses are assumed to be a Gaussian process. A combination of power spectrum and higher order spectral techniques was used by [19] to decompose the MUAP. Results were reported based on simulated EMG signals. Higher order statistics were also used by [20], [21] for decomposition of MUAPs. Satisfactory results were only obtainable for wEMG signals [20] and for reproduction of synthetic EMG signals [21].

In this paper we consider an EMG signal to be modeled by a linear time invariant (LTI) moving average (MA) system (as in (1)) with the input to the system generated by firing neuron pulses whose random times of occurrence are non-Gaussian in nature. We use a higher order statistics (HOS) based system reconstruction algorithm to estimate the typical shape of the MUAP from an EMG signal; allowing the behavior of the motor unit action potential (MUAP) to be characterized. We report on an initial assessment of the performance of the technique for estimating the appearance of the MUAP from the EMG signal. EMG signals collected from four different subjects under a variety of contraction positions and loading conditions were considered, giving the opportunity to observe the estimated MUAP shape when the muscle contraction position and/or loading changes.

This paper is organized as follows: a brief introduction to HOS and a system reconstruction technique that is based on HOS are presented in Section II. In Section III the protocol for recording the EMG signals used for MUAP estimation is described. MUAP estimation and representation techniques are discussed in Section IV. A discussion and analysis of the shape of the MUAP in different EMG signals is reported in Section V. Finally, conclusions are presented in Section VI.

II. HOS Theory for EMG Signal Analysis

Frequency domain techniques are amongst the most fundamental and useful tools in the area of signal processing. Conventional techniques are generally based on the analysis of the first- and second-order moments and cumulants (i.e., mean, correlation and variance) and their spectral representation (e.g., power spectrum). These techniques provide all the information available from the signal only if the underlying process is Gaussian and is operated on by a linear system. For non-Gaussian processes and nonlinear systems, more information can be obtained from the higher order moments and cumulants (third-order to Nth-order) and their spectral representation (higher order spectra). The second-order spectrum suppresses phase relationships, whereas information about the phase of the underlying system is available from higher order spectra [22]. Among other properties of the higher order spectra, two important ones are relevant here: 1) the higher order spectra of the sum of two or more independent sets of random processes is equal to the sum of the spectra of those random processes of the same order; and 2) the higher order spectra (≥ 2) of a Gaussian signal are theoretically equal to zero.

Higher order statistics are useful in blind deconvolution and system recovery. As they do not suppress phase information, they may be applied to nonminimum phase and nonlinear systems. As they are able to recover information about non-Gaussian signals, they are useful in systems involving non-Gaussian input signals as in the MUAPT model. In this paper we will use the second-order spectrum, the Bispectrum, to estimate the system information. The bispectrum is the most accessible of the higher order spectra as it is the simplest to compute (computational complexity increases with increasing order) and its properties have been well explored [22]–[28]. The following sections show how the bispectrum may be computed from the available system output signal [$x(n)$ in (1)] and how, assuming the model for the MUAPT described by (1), the bispectrum may be used to recover the system transfer function which describes the MUAP.

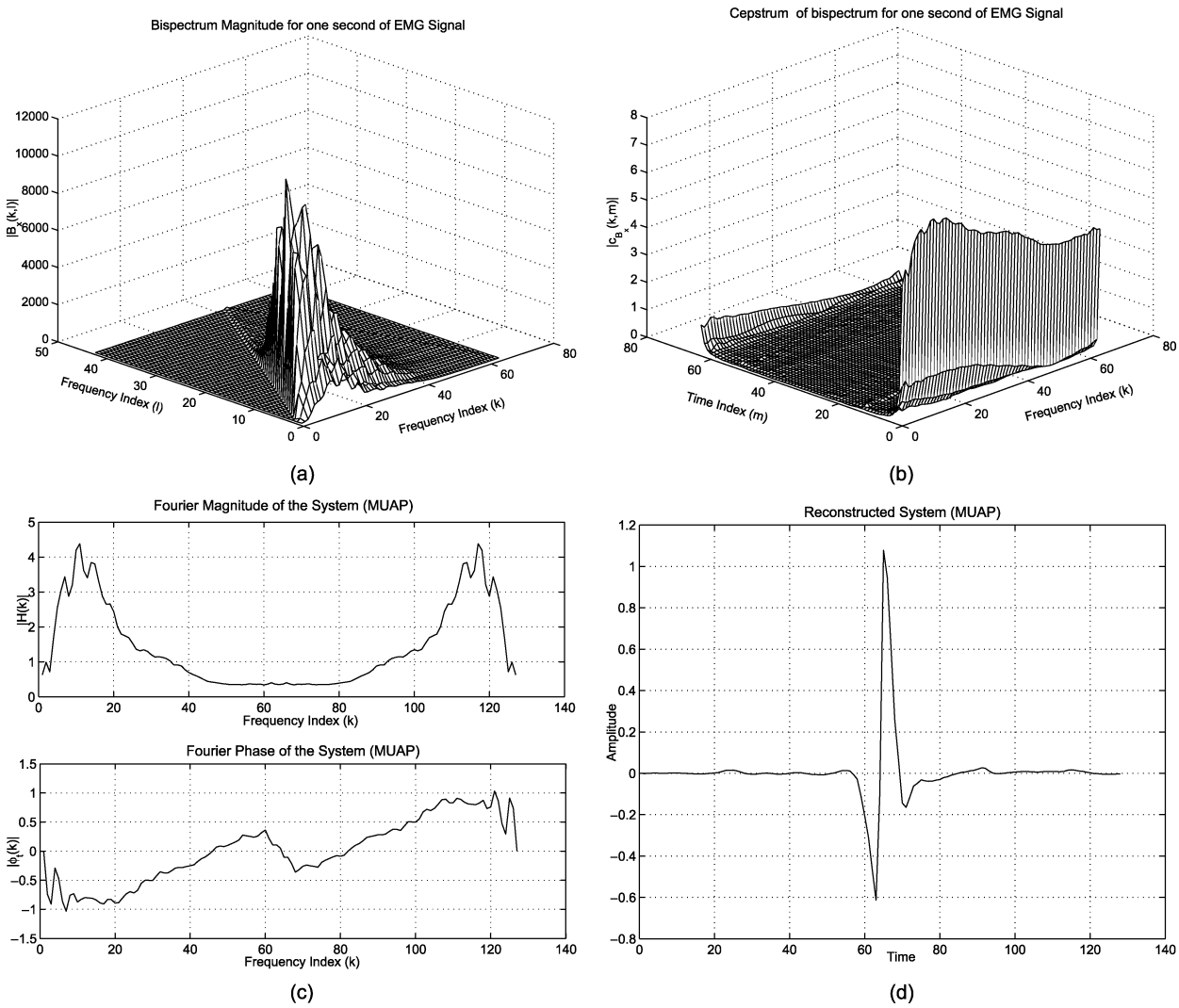

Fig. 1. Illustration of the signal processing procedure: (a) magnitude of the bispectral estimate (equation (2)) from 1 s of EMG signal. (b) Cepstrum of bispectrum (equation (5)) from 1 s of EMG signal. (c) Magnitude and phase of the system estimate [see (12)] from 1 s of EMG signal. (d) Reconstructed MUAP estimate before normalization.

A. Bispectrum

The bispectrum is the expectation of three frequencies: two direct frequency components and the conjugate frequency of the sum of those two frequencies of a random signal [22]. Knowing the Fourier frequency components, $X(k)$, of the output signal $x(n)$, the bispectrum, $B_x(k,l)$, can be estimated using the Fourier-Stieltjes representation [22]

$$B_x(k,l) = E\{X(k)X(l)X^*(k+l)\} \tag{2}$$

where $E\{\bullet\}$ denotes the statistical expectation, k,l are the discrete frequency indexes and $*$ denotes the complex conjugate. The bispectrum is complex and, therefore, it has magnitude and phase. If the output signal comes from an LTI system with a non-Gaussian white noise input signal as in (1), it can be written as [22], [23]

$$B_x(k,l) = \gamma_3^e H(k)H(l)H^*(k+l) \tag{3}$$

where γ_3^e is the skewness that is equal to the bispectrum of the input signal $e(n)$ and $H(k)$ is the transfer function of the system $h(r)$. As the Gaussian white noise is independent of the input signal and since, theoretically, the bispectrum of Gaussian white noise is zero, there is no effect from the system noise when estimating the bispectrum of the output [22], [23]. The magnitude of a typical bispectral estimate from 1 s of EMG signal (details of EMG signal acquistion are given in Section III) is shown in Fig. 1(a).

B. Cepstrum of Bispectrum System Recovery Technique

The cepstrum of bispectrum, $c_{B_x}(k,m)$, can be found by applying a 1-D inverse Fourier transform operation to the logarithm of the bispectrum (a 2-D frequency domain signal) [24], [25]

$$c_{B_x}(k,m) = F^{-1}\left[log\, B_x(k,l)\right]_l \tag{4}$$

where $F^{-1}[\bullet]_l$ denotes the 1-D inverse Fourier transform to be applied on the frequency axis l and m is the time-like index. The cepstrum of the bispectrum produces a representation of amplitude versus time versus frequency.

The cepstrum of bispectrum of any system output signal can be used to estimate the system $h(r)$ from the system output signal $x(n)$. By expressing the bispectrum of a system output signal in terms of the system transfer function as in (3), (4) can be manipulated to [25]

$$\begin{aligned} c_{B_x}(k,m) &= F^{-1}\left[log\,\gamma_3^e\right]_l + F^{-1}\left[log\,H(k)\right]_l \\ &\quad + F^{-1}\left[log\,H(l)\right]_l + F^{-1}\left[log\,H_*(k+l)\right]_l \\ &= \left[log\,\gamma_3^e\right]\delta(m) + \left[log\,H(k)\right]\delta(m) \\ &\quad + F^{-1}\left[log\,P_x(l)\right]_l \\ &= \left[log\,\gamma_3^e\right]\delta(m) + \left[log\,H(k)\right]\delta(m) + p_x(m) \end{aligned} \tag{5}$$

where $F^{-1}[\bullet]_l$ denotes the 1-D inverse Fourier transform which is applied on the frequency axis l, P_x is the power spectrum, $p_x(m) = F^{-1}[logP_x(l)]_l$ is the power cepstrum and $\delta(\bullet)$ denotes the Kronecker delta function. The cepstrum of bispectrum derived from 1 s of EMG signal is shown in Fig. 1(b). Considering only the axis $m = 0$, (5) can be expressed as

$$\begin{aligned} c_{B_x}(k,0) &= \left[log\,\gamma_3^e\right] + \left[log\,H(k)\right] + p_x(0) \\ &= \left[log\,H(k)\right] + C \end{aligned} \tag{6}$$

where $C = [log\gamma_3^e] + p_x(0)$ is a constant. Thus, (6) consists of the log of the system transfer function plus a constant. The constant can be removed by normalization, since for any blind deconvolution procedure we can only recover the system to within a scale factor [23]. Letting $k = 0$, (6) and $H(0) = 1$ gives $C = c_{B_x}$ (0,0). Thus, the system transfer function can be computed as

$$H(k) = \exp\left[c_{B_x}(k,0) - c_{B_x}(0,0)\right]. \tag{7}$$

The estimated $H(k)$ in (7) may not always be accurate as the estimated phase of the system ϕ_x [i.e., $\angle H(k)$] may vary from the true phase ϕ_t due to the fact that the true bispectrum phase (biphase) may differ by integer multiples of 2π from the estimated biphase. Therefore, it is necessary to include a phase unwrapping technique [27]. To perform phase unwrapping, we need to fit the integer values relating the true and estimated biphase as below [28]

$$\Psi_t(k,l) = \Psi_x(k,l) + 2\pi n(k,l) \tag{8}$$

where $\Psi_t(k,l)$ and $\Psi_x(k,l) = \angle B_x(k,l)$ are the true and estimated biphase values, respectively, and $n(k,l)$ is a matrix of integers.

To find the matrix of $n(k,l)$, we use a similar technique to that of [27], first, using the estimated phase of the system $\phi_x = \angle H(k)$ a shadow biphase (Ψ_s) of the bispectrum is computed as

$$\Psi_s = A_\phi \phi_x \tag{9}$$

where A_ϕ is the biphase coefficient matrix: a set of equations describing the relationship between the system phase and the resulting biphase [27]. Once the shadow biphase is found, the estimated biphase (Ψ_x) may be subtracted from it in order to recover the matrix of integers $n(k,l)$ as shown in (10) below. The result may not always be exactly on integer value and hence the elements of $n(k,l)$ are rounded to the nearest integer value

$$n(k,l) = \frac{\Psi_s - \Psi_x}{2\pi}. \tag{10}$$

Once we have the elements of $n(k,l)$, we can easily estimate the true biphase value from (8). A least squares method is then applied to estimate the true system phase

$$\phi_t = \left(A_\phi^T A_\phi\right)^{-1} A_\phi^T \left[\Psi_x + 2\pi n(k,l)\right] \tag{11}$$

where A_ϕ^T denotes the transpose of A_ϕ and $([\bullet])^{(-1)}$ denotes the matrix inverse. Now the better estimated system information can be computed by using the system's Fourier magnitude and system's Fourier phase term as

$$H(k) = |H(k)| \exp(j\phi_t) \tag{12}$$

where $|H(k)|$ is the absolute value of (7). A plot of typical system magnitude and phase as recovered by this approach from 1 s of EMG signal is shown in Fig. 1(c). Finally the inverse Fourier transform of (12) gives the time domain system information, as depicted in Fig. 1(d).

III. EMG Signal Acquisition and Processing

The EMG signals were recorded from four subjects. For each subject, two sets (using wired and surface electrodes) of EMG signals were recorded in the gait laboratory of Roessingh Research and Development, Enschede, Holland, upon ethical approval from the medical ethics committee of the Het Roessingh Hospital. Each set of signals contains two subsets of EMG signals classified on the basis of type of muscle tested—Rectus Femoris (RF) and Vastus Lateralis (VL) muscle. Each subset contains 42 EMG signals recorded at seven different contraction positions under three different loading conditions at the ankle of the subject.

A. Subjects

Four healthy male volunteers were recruited as subjects with ages ranging from 23 to 33 years old (26.2 ± 4). For each subject, the wired and surface EMG measurements were taken at the same time on each muscle. Three kinds of weight loading were tested for each subject: either no weight or by attaching 1.13 kg and 2.26 kg weights at the ankle.

B. Placement of Fine Wire and Surface Electrodes to the Muscle

The technique of EMG signal recording followed the guidelines of [30]. For RF, a line was measured between the anterior superior illiac spine and the superior border of the patella, and the fine wire electrode was inserted at 50% of the distance between both anatomical landmarks. For VL, a line was measured between the anterior superior illiac spine and the lateral border of the patella and the same type of fine wire electrode was used for EMG signal recording. The fine wire electrode used was manufactured by The California Fine Wire Company, Grover Beach, CA, and was made of stainless-steel with a diameter of

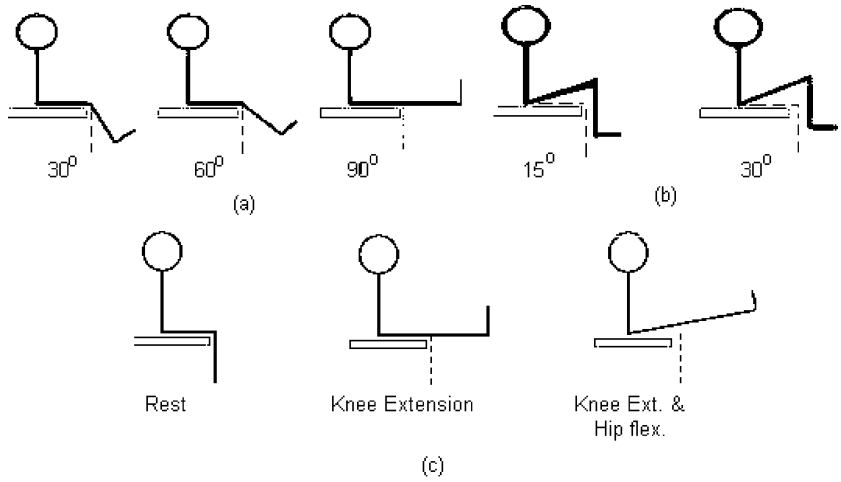

Fig. 2. The different contraction protocols. Dashed lines indicate the rest position and bold lines indicated the measurement positions. (a) Three angles (30°, 60°, and 90°) of knee extension contraction. (b) Two angles (15° and 30°) of hip flexion contraction. (c) Combined contraction protocol beginning in a resting position followed by knee extension to 90° and finally simultaneous knee extension and hip flexion. (adapted from [10]).

50 μm, 2-mm recording surface and the rest of the wire was nylon insulated.

For both RF and VL, surface electrodes were placed either side of the fine wire electrode parallel to the direction of the muscle fibers of the muscle [29]. The surface electrode was made of Ag/AgCl and square shaped with a 10 mm by 10 mm recording area, and a 22-mm interelectrode distance (manufactured by Meditrace Pellet 180, The Netherlands).

C. Different Positions for Contraction

1) Resting Protocol: All subjects began in a seated position with a knee angle of 90° (the dashed line in Fig. 2). This position is referred to here as the rest state; i.e., "no knee extension" or "no hip flexion." Two resting EMG measurements (also known as the baseline measurement) were recorded at this point with the subject in a relaxed state.

2) Vastii Protocol: Each subject had to extend the knee to angles of 30°, 60°, and 90° from the rest state [Fig. 2(a)] while wEMG and sEMG signals were simultaneously recorded from both muscles. Subsequently 1.13 kg and 2.26 kg weights were attached at the ankle and the contraction protocol was repeated using the aforementioned angles. EMGs were recorded for a 5- to 10-s period for each contraction. Two EMG measurements were taken for each angle at all weights.

3) Rectus Femoris Protocol: Subjects flexed the hip from the rest state to two angles, a low angle approximately 15° and a high angle approximately 30° [Fig. 2(b)]. This process was repeated with a 1.13 kg weight followed by a 2.26-kg weight placed around the ankle. Again, two EMG recordings were taken for each angle at all weights

4) Combination Protocol: In this case, subjects began with the leg in the resting position, after which they extended the leg to 90° knee extension and concluded with combined knee extension and hip flexion to a hip flexion angle of approximately 15° [Fig. 2(c)]. The combination contractions were performed for each of the contraction weights i.e., 0 kg (no weight), 1.13 kg, and 2.26 kg. Two EMG recordings were taken at all weights.

The order in which all muscle contractions were performed was randomized to prevent fatigue or bias in the results. Each contraction protocol was designed to elicit an EMG response from different muscles. Knee extension contractions were designed to activate the Vastii only, while the hip flexion contractions have been shown to activate RF only [30]. The combined contraction was designed to show the effect of the two different contractions on activation in the RF muscle as shown by the wEMG and sEMG. As the knee extension phase of the combined contraction was designed to activate the Vastii only, one explanation of activity in the RF muscle sEMG, which is absent from the RF wEMG signal, would be possible crosstalk from the Vastii muscles [10].

D. Acquisition of EMG Signal

On each contraction protocol, four detectors—two electrodes for the wEMG signal and two electrodes for the sEMG signal—were set up and the corresponding EMG signals were recorded simultaneously. The recording of EMG signals was performed using four channels of the "K-lab" EMG measurement system (manufactured by Biometrics Europe BV, The Netherlands). 2048 sample points were taken at a sampling rate of 2 kHz. The measurement system had an input impedance of 100 MΩ and common mode rejection ratio of 100 dB. A third-order Butterworth high pass filter (hardware filter) with cut-off frequency of 20 Hz was used on all EMG channels to increase SNR. A 12-bit analog-to-digital converter produced an output in digital format.

E. Technique of MUAP Estimation

The acquired EMG signals have been plotted using MATLAB software. From the plotted EMG signals (as an example, Fig. 3 illustrates the RF wEMG and sEMG signal of subject CAB), it is clear that the appearance and amplitude of different raw EMG signals varies with the type of contraction and level of contraction. For example, the RF muscle stays in the rest state on knee extension, as its EMG signal is similar to its EMG signal in the rest state (compare the plots labeled Rest and knee extension

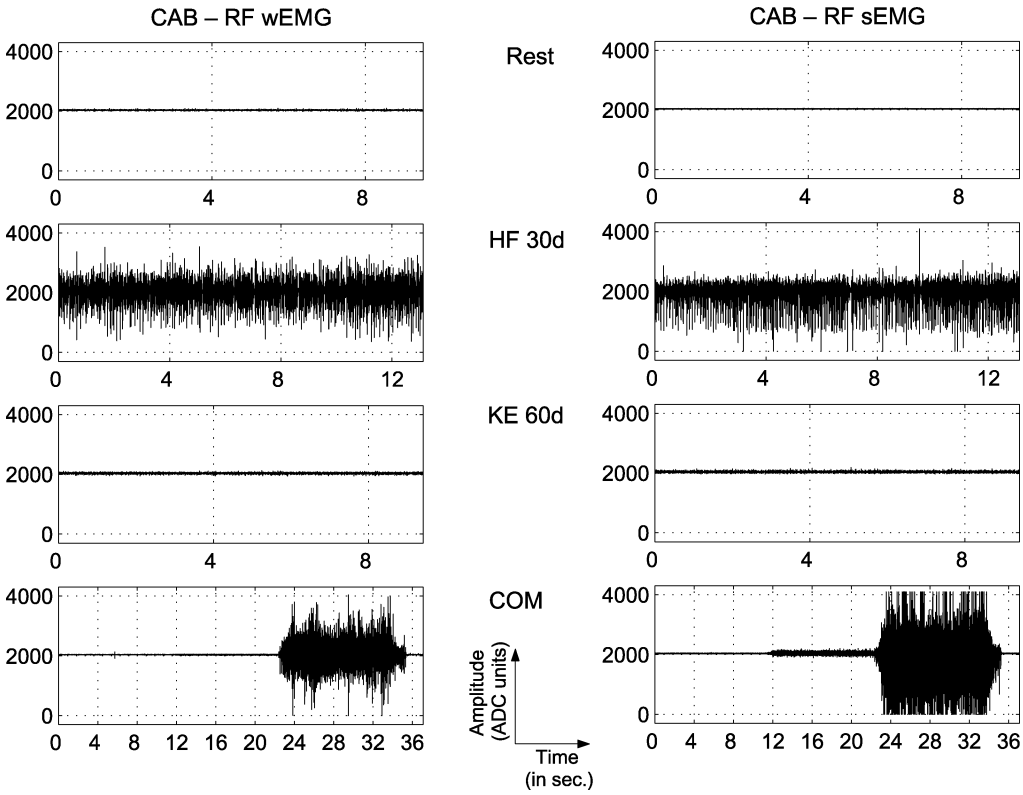

Fig. 3. wEMG and sEMG signal recorded from Rectus Femoris of subject CAB at four different contraction positions—rest, hip flexion to 30° (HF30d), knee extension to 60° (KE60d) and combined (COM).

at 60° (KE60d) of Fig. 3). In the combined contraction (COM), it is found that the wEMG signal for the RF muscle shows two different stages: rest and contraction, whereas the sEMG signal for the RF muscle shows three distinct stages: rest, a low level of contraction and a higher level of contraction. Recall that both the wEMG and sEMG signals were recorded simultaneously and the combined contraction protocol consists of three parts: rest, knee extension and hip flexion plus knee extension [see Fig. 2(c)].

In order to recover the overall shape of a MUAP, each raw EMG signal has been segmented into segments of 1-s duration where each segment contains 2048 data points. Fig. 4 shows plots of 1-s segments of EMG signals from the two different contracting muscles of subject CAB. From these plots, it is observed that the MUAP in the wEMG signal is sometimes distinguishable at a low contraction level, but it is hard to see the exact shape of the MUAP and determine the number of motor units involved. On the other hand, it becomes much more difficult to find individual MUAPs when we consider the sEMG signal of the same contracting muscle. It is also observed that the sEMG signal contains more noise that the wEMG signal.

As the raw EMG signal always contains some noise, it can be difficult to recover directly a good estimate of the MUAP shape from a raw EMG signal. By applying the cepstrum of bispectrum based system reconstruction algorithm to the EMG signal, an estimate of the MUAPs in the signal can be recovered. Bispectrum based techniques require more data to produce an estimate because of the requirement for averaging to reduce the variance of the bispectrum [22]. Therefore, the estimation of a MUAP is made from a 1-s segment of raw EMG (wEMG or sEMG) signal. The individual MUAPs within each second of raw data will each contribute information toward the estimate of the MUAP shape. A set of MUAP estimates may thus be made for each second, from first to last, of the raw signal. Due to the inherent limitations of blind deconvolution, normalized estimates of the MUAPs are computed by considering all estimated MUAPs from a given signal.

To illustrate the presentation of estimated MUAPs in any figure, we present Fig. 5 as an example where the raw signal is in the top subplot, the estimated MUAPs without normalization in the middle subplot and the estimated MUAPs normalized with respect to the whole recording in the bottom subplot of the figure. The top subplot contains three seconds of a raw EMG signal (i.e., 3X2048 data points). The middle subplot shows three MUAPs where each MUAP has been estimated from 1 s of the raw signal: i.e., the first MUAP has been estimated from the raw EMG signal of the first second; the second MUAP has been estimated from the raw EMG signal of the second and so on. The last subplot is the normalized form of the middle subplot. On the x axis of each subplot is displayed the time points of the raw signal from which the MUAPs have been estimated and the y axis displays the amplitude of the raw signal (top subplot) and of the estimated MUAPs (middle and bottom subplots). Note that the time-scale in the middle and bottom subplots is for delineating the contribution of each second of the raw EMG signal and the presence of an estimated MUAP at a particular time on the time scale does not indicate that the raw EMG signal necessarily contains a MUAP at that exact time instant.

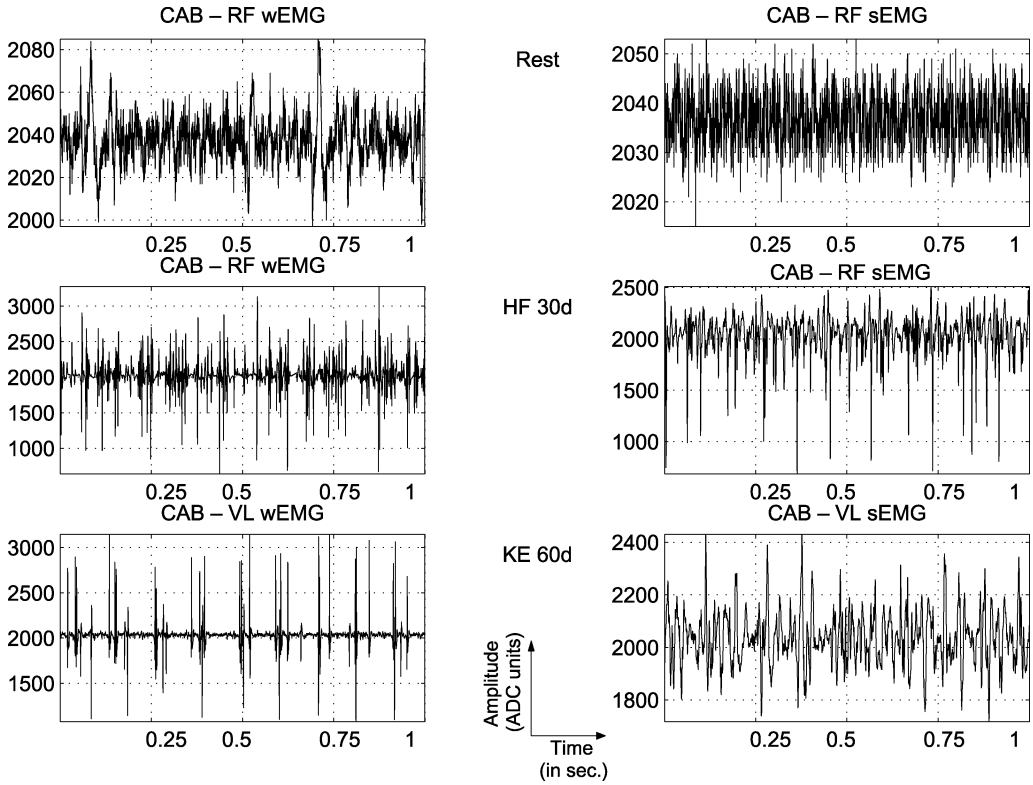

Fig. 4. wEMG and sEMG signal recorded from the Rectus Femoris of subject CAB at rest, hip flexion to 30° (HF30d), and knee extension to 60° (KE60d).

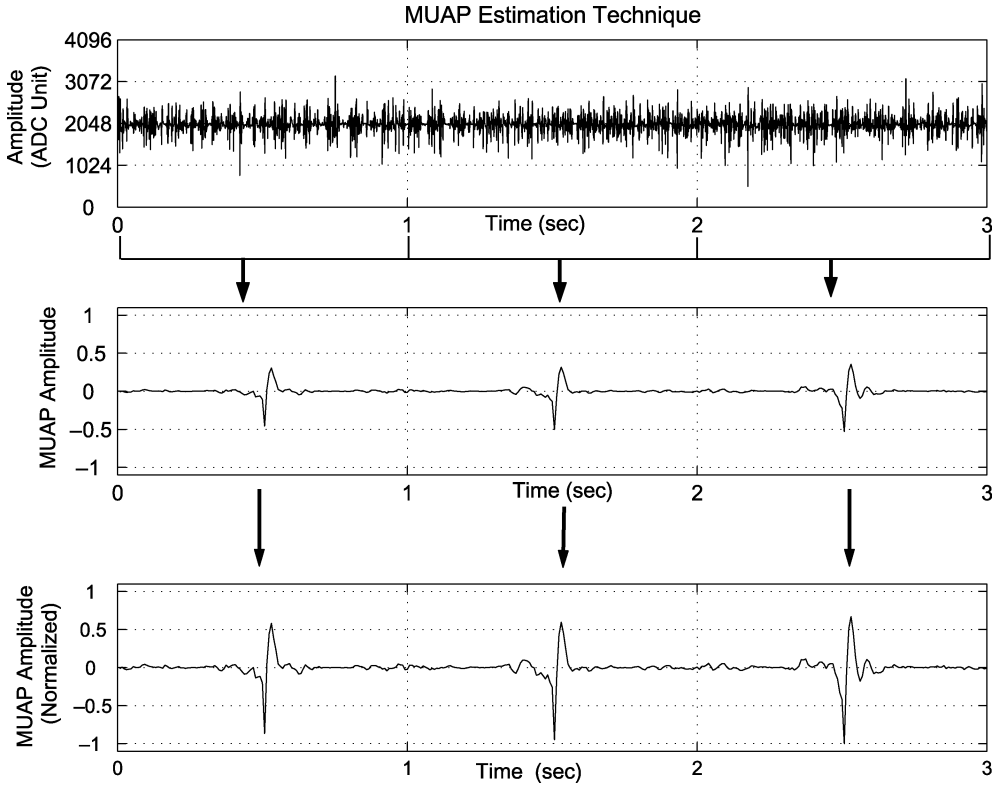

Fig. 5. MUAP estimation technique. Raw wEMG signal (top), corresponding estimated MUAP (middle) and normalized form of estimated MUAPs (bottom). The x-axes of all subplots are the time scale of the original recording (in seconds). The y axis shows the amplitude of raw data (top), estimated MUAP (middle) and normalized MUAP (bottom).

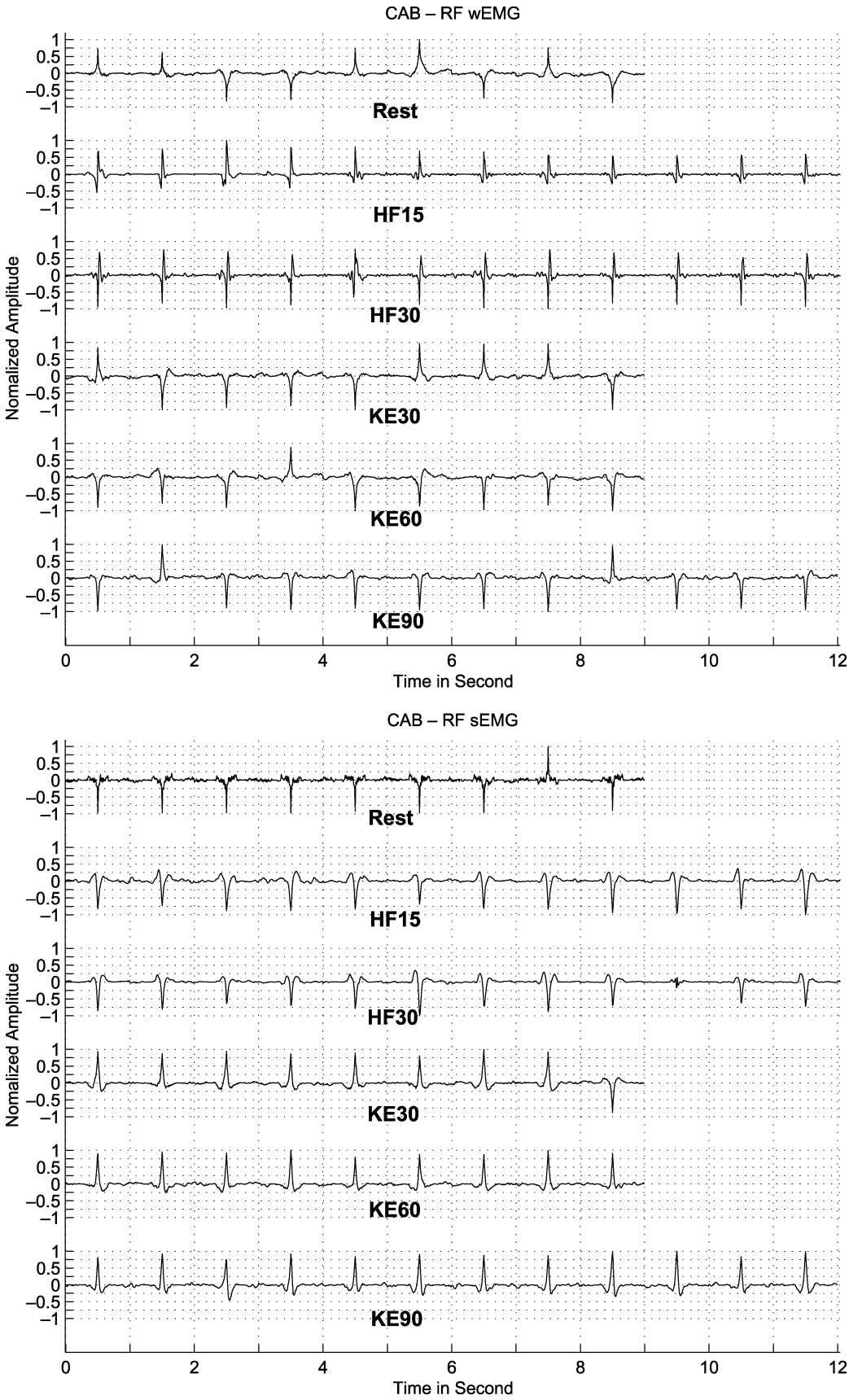

Fig. 6. Appearance of MUAP in wEMG (top) and sEMG (bottom) signals of Rectus Femoris muscle (subject-CAB). Both subplots show the estimated MUAPs at five contraction positions: rest, hip flexion 15° (HF15), hip flexion 30° (HF30), knee extension 30° (KE30), knee extension 60° (KE60), knee extension 90° (KE90).

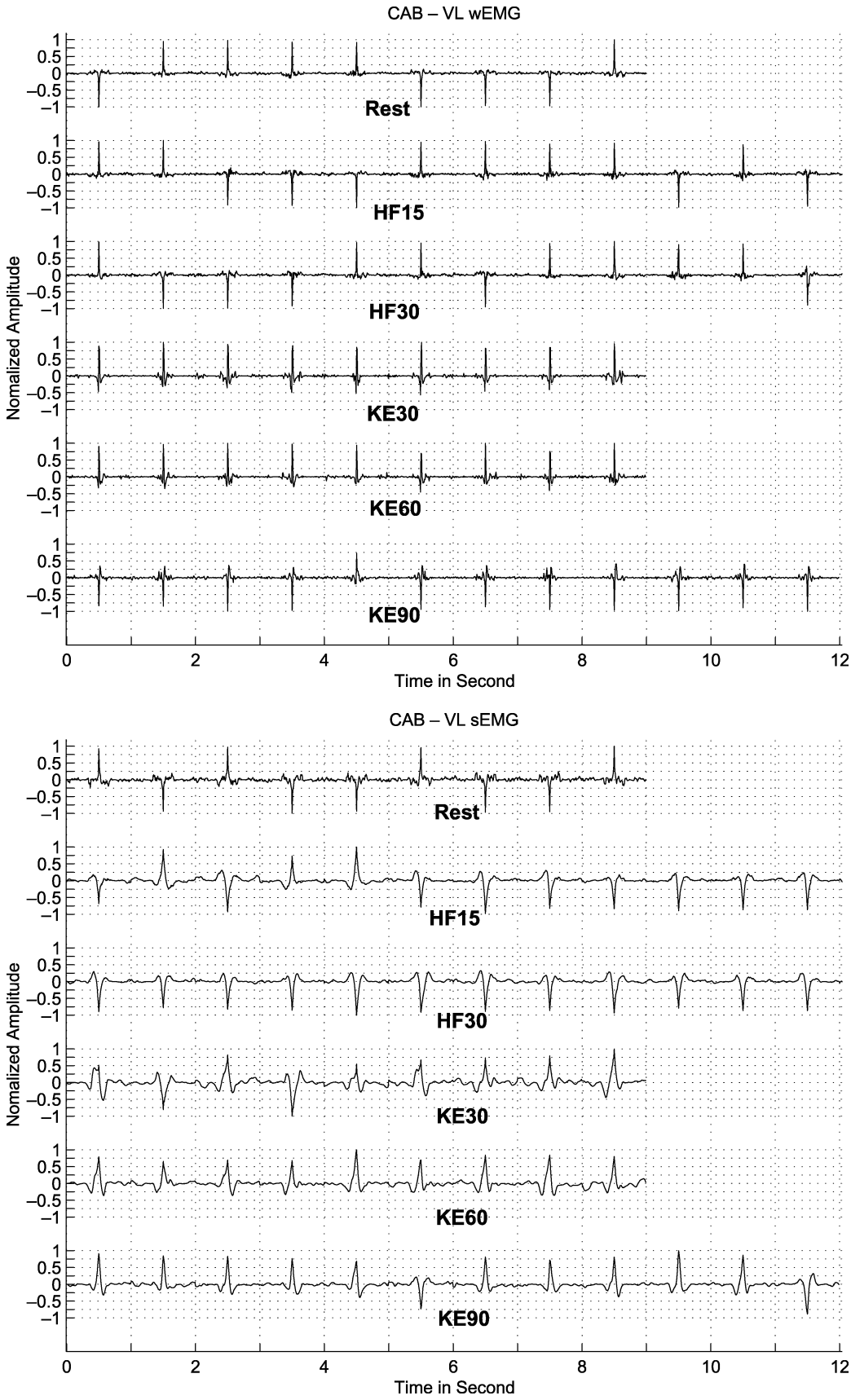

Fig. 7. Appearance of MUAP in wEMG (top) and sEMG (bottom) signals of Vastus Lateralis muscle (subject-CAB). Both subplots show the estimated MUAPs at five contraction positions: rest, hip flexion 15° (HF15), Hip flexion 30° (HF30), knee extension 30° (KE30), knee extension 60° (KE60), knee extension 90° (KE90).

TABLE I
MUAP CHARACTERISTICS OF RF AND VL MUSCLE AT DIFFERENT CONTRACTION POSITIONS

Contraction Position and Signal Type	MUAP Shape (contained MUAP phase†)	Orientation of MUAP Peak (in a single recording)	Evidence of Crosstalk
Rest	spike-like‡	both sides of zero	–
Hip Flexion 15°			
RF wEMG	all phases (R + O + U)	one side of zero	no
RF sEMG	all phases (R + O + U)	one side of zero	no
VL wEMG	spike-like‡	both sides of zero	no
VL sEMG	all phases (R + O + U)	mostly 1 side of zero	some
Hip Flexion 30°			
RF wEMG	all phases (R + O + U)	one side of zero	no
RF sEMG	all phases (R + O + U)	one side of zero	no
VL wEMG	spike-like‡	both sides of zero	no
VL sEMG	all phases (R + O + U)	one side of zero	yes
Knee Extension 30°			
RF wEMG	spike-like‡	both sides of zero	no
RF sEMG	spike-like‡	one side of zero	yes
VL wEMG	all phases (R + O + U)	mostly 1 side of zero	no
VL sEMG	all phases (R + O + U)	one side of zero	no
Knee Extension 60°			
RF wEMG	spike-like‡	mostly 1 side of zero level	some
RF sEMG	spike-like‡	one side of zero level	yes
VL wEMG	all phases (R + O + U)	one side of zero level	no
VL sEMG	all phases (R + O + U)	one side of zero level	no
Knee Extension 90°			
RF wEMG	spike-like‡	mostly 1 side of zero level	yes
RF sEMG	spike-like‡	one side of zero level	yes
VL wEMG	all phases (R + O + U)	one side of zero level	no
VL sEMG	all phases (R + O + U)	one side of zero level	no

† MUAP shape has been expressed in three phases: Rest phase = R, Overshot phase = O and Undershot phase = U
‡ Spike-like means the presence of two phases: rest + undershot or rest + overshot

IV. RESULTS

Following the procedure described above, MUAPs have been estimated from the simultaneously recorded wEMG and sEMG signal of the RF and VL muscles of the four subjects. Here we present the results of estimated MUAPs for one subject (CAB) only. Figs. 6 and 7 display the estimated MUAPs for six contraction positions: rest, hip flexion 15° (HF15), hip flexion 30° (HF30), knee extension 30° (KE30), knee extension 60° (KE60) and knee extension 90° (KE90). The behavior of MUAPs in the different contraction positions has been summarized in Table I. To observe the behavior of MUAPs during the combined contraction we estimated the MUAP from the three separate stages of the EMG and plotted the results in Fig. 8. We also estimated the MUAPs from the EMG signal when the subjects have different loads at the ankle. Fig. 9 displays one example of the MUAPs' behavior which were estimated from the wEMG and sEMG signals of the RF muscles of subject CAB with different weights at the ankle.

In MUAP observation and analysis, the shape of the MUAP has been described by the presence and the duration of three phases—rest phase, overshot phase (depolarizing phase), and undershot phase (repolarizing phase). The behavior of the MUAP at different contraction positions is noted below.

A. MUAP in the EMG Signal With Subject at Rest

The MUAP of rest muscle can be seen in the first sequence in both subplots of Figs. 6 and 7. From these MUAPs the following points can be noted.

1) The shape of the MUAP in resting muscle EMG signal is impulse-like and the peak may appear randomly to both sides (positive and negative) of zero level.
2) The shape and appearance of the estimated MUAPs are similar in both the wEMG and sEMG signal.

These characteristics are summarized in Table I.

B. MUAP in the EMG Signal With Subject Holding Hip Flexion

The MUAPs at this contraction position (see Fig. 2(b): hip flexion to 15° and 30°) are displayed in the second and third sequences in each of the subplots of Figs. 6 and 7. The behavior of estimated MUAPs can be described as follows and are also summarized in Table I.

1) The MUAPs in the RF wEMG signal confirm that the RF muscle is contracting because: a) the MUAPs have three phases (rest, overshot and undershot phase) and b) the peaks of all MUAPs appear to only one side of the base line (zero level).
2) The MUAPs in the RF sEMG signal also show that the muscle is contracting as it behaves similarly to the above.
3) The MUAPs in the VL wEMG signal confirms that the muscle stays at rest in hip flexion as the MUAPs show similar behavior to the resting muscle MUAP (see resting muscle behavior in Table I or the first sequence in Figs. 6 and 7).
4) The MUAPs in the VL sEMG signal do not always show the resting state shape. At a low angle of hip flexion the

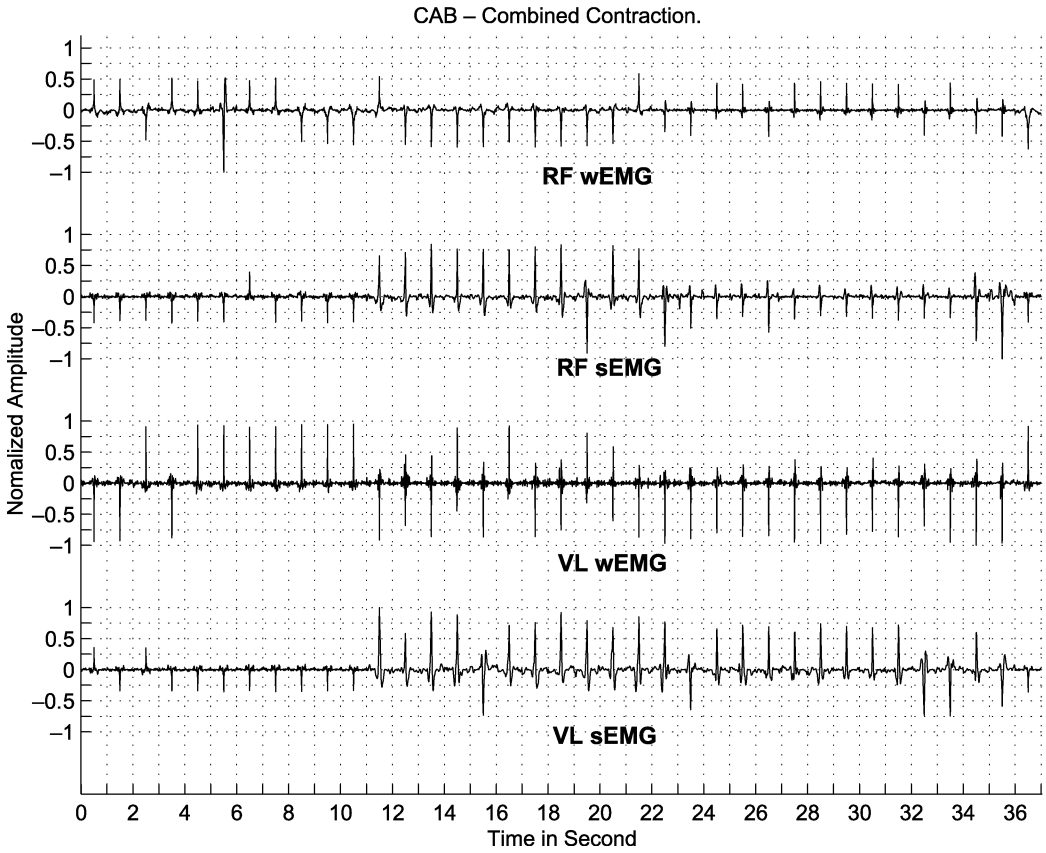

Fig. 8. Appearances of MUAP in Rectus Femoris and Vastus Lateralis muscle (subject-CAB) for the combined contraction. The figure illustrates the MUAPs estimated from Rectus Femoris wEMG (RF-wEMG), Rectus Femoris sEMG (RF-sEMG), Vastus Lateralis wEMG (VL-wEMG) and Vastus Lateralis sEMG (VL-sEMG).

MUAP is similar to the rest state MUAP, but at a high angle of hip flexion the peak amplitude of the MUAPs appear mostly to one side of zero level.

The appearance of the MUAP in the VL sEMG signal at a high angle of hip flexion could be a superimposing effect from other muscles (crosstalk) or could indicate contraction (low level contraction). Furthermore, the appearance of MUAPs in the VL sEMG signal are similar to the appearance of MUAPs in the RF sEMG signal (see Table I or compare the sEMG subplots in Figs. 6 and 7). Therefore, for this case, this appearance indicates the possibility of the presence of a crosstalk signal in the VL muscle due to RF muscle contraction.

C. MUAP in the EMG Signal With Subject Holding Knee Extension

The fourth, fifth and sixth sequences in each subplot of Figs. 6 and 7 display the average appearance of MUAPs at this contraction position (Fig. 2(a)—knee extended at 30°, 60° and 90°). The behavior of the estimated MUAPs are described below and also summarized in Table I.

1) As expected, the behavior of the MUAPs in the wEMG and sEMG signals from the VL muscle show the appearance of a contracting muscles MUAP, having three phases and with the MUAP peak appearing mostly to one side of zero level.
2) The MUAPs in the RF sEMG signal would suggest that the muscle is not at rest. Thus, there is evidence of a crosstalk signal due to VL muscle contraction as the appearance of the MUAPs in the RF sEMG signal and the VL sEMG at this contraction position are similar.
3) The MUAPs in the RF wEMG signal appear similar to the baseline Rest state, but as the angle of knee extension increases more of the behavior of nonresting muscle MUAPs becomes apparent: the peak of the MUAPs appear to one side of zero level. However, there is not a strong appearance of three phases of MUAP. This appearance may indicate one of two things: 1) the influence of another contracting muscle i.e., a crosstalk signal due to a neighboring muscle but not from the VL muscle because it is not similar to the appearance of the MUAP as it is estimated from the VL muscle; 2) the RF muscle actually is contracting at this time (at a low level).

D. MUAP in the EMG Signal When Subject Executes a Combination Contraction

Fig. 8 displays the average appearance of MUAPs during the combined contraction protocol [Fig. 2(c)]. Recall that the EMG signal recorded from a combination contraction has three stages: 1) rest state (from 1st to the 11th second in this case); 2) knee extension (from 12th to the 22nd second); 3) knee extension plus

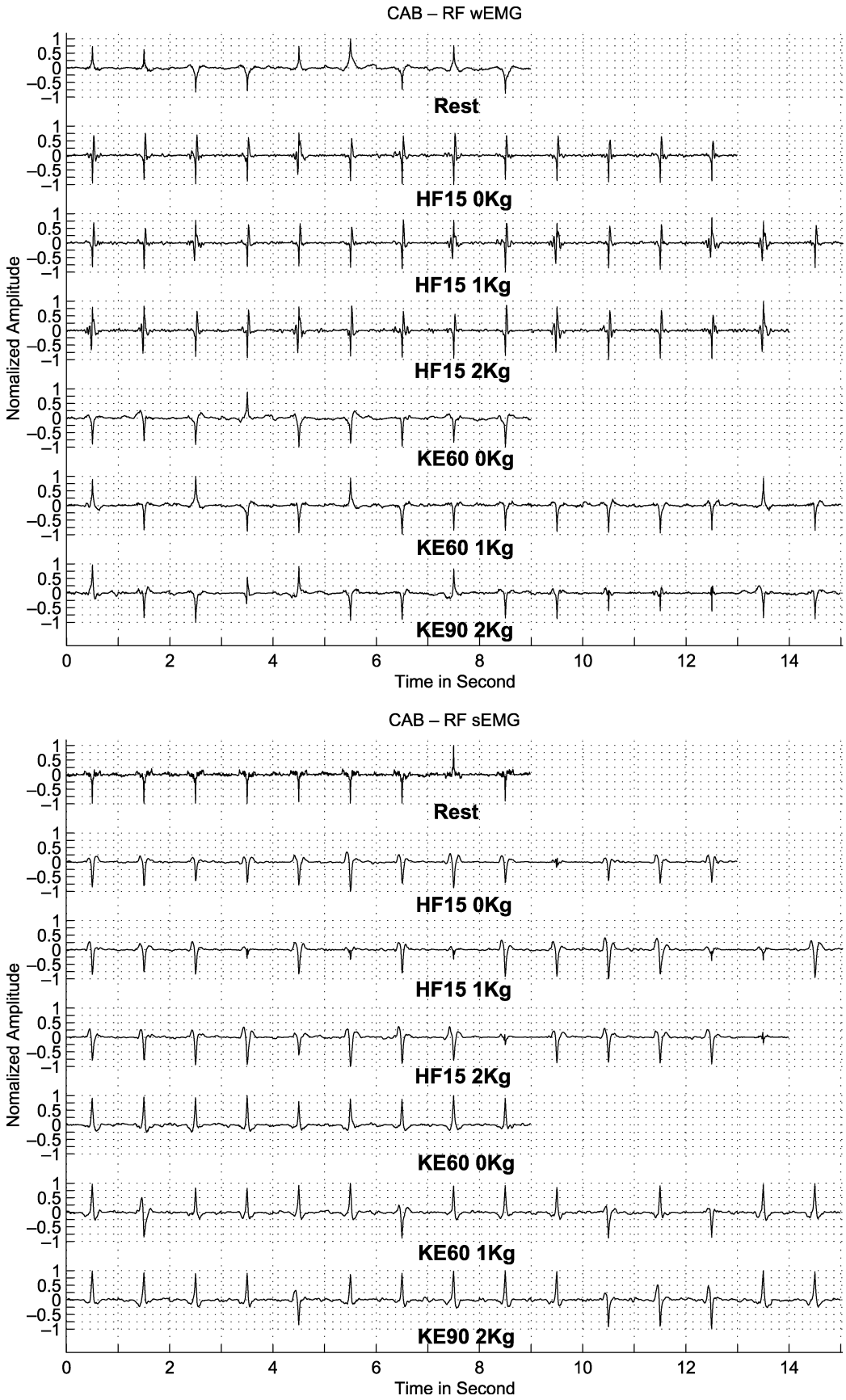

Fig. 9. MUAPs estimated from (a) wEMG and (b) sEMG signal of the RF muscle when subject CAB has either no load (0 kg), 1.13 kg (1 kg) and 2.26 kg (2 kg) attached at the ankle and contraction positions are hip flexion to 15° (HF15) and knee extension to 60° (KE60).

hip flexion (from the 23rd to the 36th second in this case). Thus, in the figure, the first 11 second along the time axis show the MUAPs extracted from the rest state, the 12th to the 22nd second time points show the MUAPs extracted from the knee extension stage and the 23rd to the 36th second time points show the MUAPs extracted from the knee extension plus hip flexion stage. Comparing this sequence with Figs. 6 and 7 (also with Table I), the first two stages (the rest state and the knee extension) are distinguishable. The appearance of MUAPs in the third part of these sequences when the knee was extended and the hip was flexed has the following features.

1) In the wEMG signals for each muscle, the dominant appearance is of course of the MUAP associated with the contraction which the muscle is performing. Thus, in the RF wEMG signal during the combined contraction, the MUAP appearance is similar to the appearance of MUAPs in the RF wEMG signal during hip flexion. Similarly, in the VL wEMG signal, the MUAPs appear similar to the appearance of MUAPs in the VL wEMG signal during knee extension.
2) During this third part of the combined contraction, there is not much evidence of crosstalk from the RF muscle in the sEMG signal taken from the VL muscle. The MUAPs in the sEMG signal from the VL muscle show a similar appearance to the MUAPs of knee extension alone (e.g., as seen in Figs. 6 and 7). On the other hand, in the RF muscle the MUAPs appear to be a sum of MUAPs characteristic of hip flexion and knee extension (i.e., with low amplitude of MUAP with clear overshot and undershot in MUAP). Thus there is evidence of crosstalk in the RF sEMG signal due to the contracting VL muscle.

E. Comparison of Estimated MUAP—Subject With and Without Load

In this case, the MUAPs were estimated from the EMG signal acquired when the subjects were seated in six different contraction positions as before and at the same time a load (1.13 kg or 2.26 kg) was attached to the ankle. Fig. 9 displays the MUAP estimated from the wEMG and sEMG signals, respectively, of the RF muscle of CAB. Each subplot shows the MUAPs for three contraction positions with three different loads ["no load (0 kg)," "1.13 kg load (1 kg)," or "2.26 kg load (2 kg)"] at the subject's ankle (where the term in brackets denotes the abbreviation used in the figure). The contraction positions are: rest, hip flexion to 15° and knee extension to 60°. Recall that the estimated MUAPs are presented here in normalized form and the normalization is made with respect to the whole recording.

From all the subplots, it is clear that the shape of MUAPs remains broadly similar if the subject increases effort: either to increase the angle at which the knee or hip is held or because of increased loading at the ankle. Due to the normalization inherent in the signal processing, it is not possible to compare the amplitudes of the recovered MUAPs. The unchanging shape of the MUAPs suggests that the effect of increased effort due to, for example loading at the ankle, may have another impact in the EMG signal, such as increasing the frequency of neuron firing pulses and thus the recruitment of motor units.

V. Discussion and Conclusion

The mathematical model adopted in this paper of the EMG signal is of the output of a LTI system whose input is non-Gaussian white noise. Based on this model, we have used our cepstrum of bispectrum based system reconstruction algorithm to estimate MUAPs from a range of real EMG signals obtained during isometric contraction. Our results show that the cepstrum of bispectrum approach can recover good estimates of MUAPs from both wEMG and sEMG signals.

Following on the successful work of [15], [16], there now exist many EMG decomposition programs [31] but these are mainly successful only for wEMG signals and many such programs require the intervention of a human operator [31]. An early use of higher order statistics based approaches to recovery of MUAPs from the sEMG signal was by Yana *et al.* [19]. However, their approach was only applied to simulated sEMG signals. Other workers have tried a variety of approaches to the decomposition and recovery of MUAPs from the EMG with only varying success. For example the approach of [17] is simply a first step to locating the MUAPs in an sEMG signal. Approaches described in [18], [20], and [21] have only been successful on wEMG signals or on simulated sEMG signals. In [32] a parametric modeling approach to sEMG decomposition is described which reproduces the appearance of heavily overlapped MUAPs in the sEMG. However, this approach does not allow visualization of the individual MUAPs which are contributing to the overlapped MUAP. The best success in recovery of individual MUAPs from the sEMG has been by use of expensive specialized electrodes and associated spatial filtering [33]. Our approach produces MUAP estimates which are comparable in quality to those produced by the multiple electrode approach but without the need for specialized equipment.

The concentric-ring electrode approach can distinguish individual MUAP trains and we do not claim that our approach can achieve this. It can simply reveal the average appearance of the MUAP in the muscle. It is well established that the average shape of MUAPs in any EMG signal conveys information about the contracting muscle [31]. For example, the shape of the MUAP may change if the number of motor units involved changes, in other words it reflects motor unit recruitment. In the experiments described, the detector positions were fixed for all contractions and wEMG and sEMG were recorded simultaneously. Our results clearly show, from the different appearance of the MUAPs in the wEMG and sEMG from the same muscle, the effect of motor unit recruitment.

Our results indicate that the resting muscle's wEMG or sEMG contains a train of impulse-like MUAPs whose peaks are oriented to both sides of zero level. In fact, there is no involvement of motor unit in the resting muscle and the observed impulse-like MUAP estimated from the resting muscle's EMG signal, is the effect of noise and can be considered as a baseline signal which is a "signature" of a resting muscle. Our results further suggest that the MUAPs tend to be oriented to one side of zero level when the muscle is contracting. The particular direction they point depends on the orientation of the electrodes with respect to the active motor units.

A contracting muscle as expected produces MUAPs where each MUAP has three phases. As contraction strength increases,

the shape of the MUAP may change due to increased motor unit recruitment as noted above. Similarly, the duration of the undershot and overshot phases in MUAPs in the sEMG signal are longer than in those of the wEMG signal. This longer duration indicates the involvement of more MUAPs being detected due to the nature of surface detection in the sEMG signal.

It was also observed that the shape of the estimated MUAPs remains the same when EMG signals are recorded with increasing loads at a subject's ankle. Due to the normalization inherent in the signal processing, it is not possible to compare the amplitudes of the recovered MUAPs. The increasing effort by the muscle cannot be directly detected by our technique without additional processing. For example, with further processing by inverse filtering, our approach can be used to recover the firing instants [33] which can then be used to explore the effects of increased loading.

Our approach is also able to detect crosstalk in one muscle due to activity in another muscle. It can do this not just because it is possible to detect activity in the sEMG when there is no activity in the wEMG [11], but also because it is possible to compare the appearance of MUAPs in the two muscles. For example, the appearance of MUAPs in the VL sEMG signal during hip flexion are similar to the appearance of MUAPs in the RF sEMG signal (the muscle which is actually producing the hip flexion) so we can conjecture that there is a crosstalk signal appearing. The orientation of the MUAPs may also change in the case of crosstalk, for example as occurs in the RF sEMG signals during knee extension, under the influence of crosstalk from the VL muscle.

In conclusion, we believe that our signal processing approach to MUAP recovery from wEMG and sEMG is useful because it provides a quick (real time), cheap software-based solution to visualising MUAPs. With further processing our procedure can also be used to recover firing instants and firing rates.

REFERENCES

[1] C. J. DeLuca, "Physiology and mathematics of myoelectric signals," *IEEE Trans. Biomed. Eng.*, vol. BME-26, no. 6, pp. 313–325, Jun 1979.

[2] D. Stashuk, "EMG signal decomposition: how can it be accomplished and used?," *J. Electromyogr. Kinesiol.*, vol. 11, pp. 151–173, 2001.

[3] P. A. Kaplanis, C. S. Pattichis, L. J. Hadjileontiadis, and S. M. Panas, "Bispectral analysis of surface EMG," in *Proc. 10th Mediterranean Electrotechnical Conf.*, vol. II, 2000, pp. 770–773.

[4] J. Kollmitzer, G. R. Ebenbichler, and A. Kopf, "Reliability of surface electromyographic measurements," *Clin. Neurophysiol.*, vol. 110, pp. 725–734, 1999.

[5] F. B. Stulen and C. J. DeLuca, "Frequency parameters of the myoelectric signal as a measure of muscle conduction velocity," *IEEE Trans. Biomed. Eng.*, vol. BME-28, no. 7, pp. 515–523, Jul. 1981.

[6] E. A. Clancy, E. L. Morin, and R. Merletti, "Sampling, noise reduction and amplitude estimation issue in surface electromyography," *J. Electromyogr. Kinesiol.*, vol. 12, pp. 1–16, 2002.

[7] C. J. De Luca and E. J. Van Dyk, "Derivation of some parameters of myoelectric signals recorded during sustained constant force isometric contractions," *Biophysical J.*, vol. 15, pp. 1167–1180, 1975.

[8] A. A. Rodriquez and J. C. Agre, "Electrophysiologic study of the quadriceps muscles during fatiguing exercise and recovery: a comparison of symptomatic and asymptomatic postpolio patients and controls," *Arch. Phys. Med. Rehab.*, vol. 72, pp. 993–997, 1991.

[9] H. Onishi, R. Yagi, K. Akasaka, K. Momose, K. Ihashi, and Y. Handa, "Relationship between EMG signals and force in human vastus lateralis muscle using multiple bipolar wire electrode," *J. Electromyogr. Kinesiol.*, vol. 10, pp. 59–67, 2000.

[10] C. A. Byrne, "An investigation of ambulatory electromyography for rehabilitation application," M.Sc thesis, Univ. Limerick, Limerick, Ireland, 2003.

[11] A. Nane, C. Byrne, and H. Hermens, "Is rectus femoris really a part of quadriceps? assessment of rectus femoris function during gait in able-bodied adults," *Gait and Posture*, 2003, to be published.

[12] K. Ogino, "Spectrum analysis of surface electromyogram (EMG)," in *Proc. IEEE Int. Conf. Acoustics, Speech Signal Processing*, 1983, pp. 1114–1117.

[13] J. V. Basmajian and C. J. DeLuca, *Muscles Alive—The Functions Revealed by Electromyography*. Baltimore, MD: Williams & Wilkins, 1985.

[14] D. Dumitru, J. C. King, and S. D. Nandedkar, "Motor unit action potentials recorded with concentric electrodes: physiology implications," *J. Electromyogr. Clin. Neurophysiol.*, vol. 105, pp. 333–339, 1997.

[15] K. C. McGill, K. Cummins, and L. Dorfman, "Automatic decomposition of the clinical electromyogram," *IEEE Trans. Biomed. Eng.*, vol. BME-32, pp. 470–477, 1985.

[16] D. W. Stashuk, "Mean, median and mode estimation of motor unit action potential templates," in *Proc. Int. Conf. IEEE Engineering in Medicine and Biology Society*, 1996, pp. 1498–1499.

[17] Z. Xu and S. Xiao, "Digital filter design for peak detection of surface EMG," *J. Electromyogr. Kinesiol.*, vol. 10, pp. 275–281, 2000.

[18] Y. Zhou, R. Chellappa, and G. Bekey, "Estimation of intramuscular EMG signals from surface EMG signal analysis," in *Proc. IEEE Int. Conf. Acoustics, Speech and Signal Processing*, vol. 11, 1986, pp. 1805–1808.

[19] K. Yana, H. Marushima, H. Mino, and N. Takeuchi, "Bispectral analysis of filtered impulse processes with applications to the analysis of bioelectric phenomena," in *Proc. Workshop Higher-Order Spectral Analysis*, 1989, pp. 140–145.

[20] D. Zazula, D. Korosec, and A. Sostaric, "Computer-assisted decomposition of the electromyograms," in *Proc. 11th IEEE Symp. Computer-Based Medical System*, 1998, pp. 26–31.

[21] D. Zazula, "Higher-order statistics used for decomposition of SEMGs," in *Proc. 12th IEEE Symp. Computer-Based Medical Systems*, 1999, pp. 72–77.

[22] C. L. Nikias and M. R. Raghuveer, "Bispectrum estimation: a digital signal processing framework," *Proc. IEEE*, vol. 75, no. 7, pp. 869–891, Jul. 1987.

[23] C. L. Nikias and A. P. Petropulu, *Higher-Order Spectral Analysis: A Nonlinear Signal Processing Framework*. Englewood Cliffs, NJ: PTR Prentice-Hall, 1993.

[24] S. Shahid and J. Walker, "The complex cepstrum of bispectrum for system reconstruction with application to sEMG signal," in *Proc. Irish Signals and Systems Conf.*, 2003, pp. 230–235.

[25] S. Shahid, "Higher order statistics techniques applied to EMG signal analysis and characterization," Ph.D. thesis, Univ. Limerick, Limerick, Ireland, 2004.

[26] T. S. Rao and M. M. Gabr, "A Test for Linearity of Stationary Time Series," *J. Time Ser. Anal.*, vol. 1, no. 1, pp. 145–158, 1980.

[27] M. Rangoussi and G. B. Giannakis, "FIR modeling using log-bispectra: weighted least-squares algorithms and performance analysis," *IEEE Trans. Circuits Syst.*, vol. 38, no. 3, pp. 281–296, Mar. 1991.

[28] J. C. Marron, P. P. Sanchez, and R. C. Sullivan, "Unwrapping algorithm for least-squares recovery from the modulo 2π bispectrum phase," *J. Opt. Soc. Am. A*, vol. 7, no. 1, pp. 14–20, Jan. 1990.

[29] H. J. Hermens, B. Freriks, R. Merletti, D. Stegeman, J. Bok, G. Rau, C. Disselhorst-Klug, and G. Hagg, "European Recommendations for Surface Electromyography, Results of the Seniam Project," Roessingh Research and Development, The Netherlands, 1999.

[30] S. Ounpuu, P. DeLuca, K. Bell, and R. Davis, "Using surface electrodes for the evaluation of the rectus femoris, vastus medialis and vastus lateralis muscles in children with cerebral plasy," *Gait Posture*, vol. 5, pp. 211–216, 1997.

[31] D. Farina, A. Crosetti, and R. Merletti, "A model for the generation of synthetic intramuscular EMG signals to test decomposition algorithms," *IEEE Trans. Biomed. Eng.*, vol. 48, no. 1, pp. 66–77, Jan. 2001.

[32] D. Korosec, C. Martinez, and D. Zazula, "Parametric modeling of EMG signals," in *Proc. 18th Annu. Int. Conf. IEEE EMBS*, 1996, pp. 1470–1471.

[33] D. Farina and C. Cescon, "Concentric-ring electrode systems for noninvasive detection of single motor unit activity," *IEEE Trans. Biomed. Eng.*, vol. 48, no. 11, pp. 1326–1334, Nov. 2001.

[34] S. Shahid, J. Walker, G. Lyons, and C. A. Byrne, "Characterization of neuron firing pulses in electromyographic signal," in *Proc. 17th Int. EURASIP Conf. BIOSIGNAL 2004*, 2004, pp. 72–74.

Shahjahan Shahid was born in Bogra, Bangladesh. He received the B.Sc. and M.Sc. degree in applied physics and electronics from the University of Rajshahi, Rajshahi, Bangladesh, in 1988 and 1990, respectively. He received the Ph.D. degree in electronics and computer engineering from the University of Limerick, Limerick, Ireland, in 2004.

During 1991 to 1997, he was with the Bangladesh Atomic Energy Commission as a Scientific Officer. He is currently with g.tec Guger Technologies OEG, Graz, Austria working on bio-signal processing. His main research interests lie in the area of higher order statistical signal processing and its applications in estimation theory, bio-signal analysis and medical instrumentation.

Jacqueline Walker (S'91–M'97) was born in London, U.K. She received the B.A. and the B.E. (First Class Honors) degrees, both from the University of Western Australia, Perth, in 1987 and 1992, respectively. She received the Ph.D. degree from Curtin University of Technology, Bentley, Australia, in 1997.

During 1996–1997, she was employed as a Research Engineer by the Australian Telecommunications Research Institute. In November 1997, she joined the Department of Electronic and Computer Engineering at the University of Limerick, Limerick, Ireland, as a Lecturer. Her research interests include signal processing applied to biomedical, speech and music signals with particular interest in blind deconvolution and blind source separation.

Dr. Walker is a member of the Institution of Electrical Engineers.

Gerard M. Lyons received the B.E. degree (First Class Honors) in electrical engineering in 1980 and the M.Eng.Sc. degree in microelectronics in 1982 from University College, Cork, Ireland. He received the Ph.D. degree in biomedical engineering from the National University of Ireland, Galway, in 2000.

From 1985 to 1990 Dr. Lyons worked in the semiconductor industry in the Santa Clara Valley and Monterey Peninsula in California. He returned to Ireland in 1990 and joined the University of Limerick as a member of faculty and is currently a Senior Lecturer in Electronic and Computer Engineering, Assistant Dean, Research, College of Informatics and Electronics and Director of the Biomedical Electronics Laboratory at the university. His primary research interests are gait rehabilitation using FES, mobility assessment of the elderly, and use of computer-based biofeedback techniques for rehabilitation applications.

Ciaran A. Byrne was born in Drogheda, Ireland, in 1977. He received the B.Sc. degree in sport and exercise science from the University of Limerick, Limerick, Ireland, in 1999. In 2002, he received the M.Sc. degree from the same institution.

He is currently a Research Scientist for BioMedical Research Ltd., an Irish company that develops muscle stimulation products for the sports, health, and medical markets. His research interests include muscle stimulation, EMG, and strength and conditioning. He is a Certified Strength and Conditioning Specialist and is a member of the ESSAI.

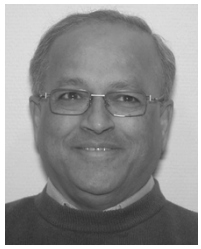

Anand Vishwanath Nene was born in Bombay, India. He received the M.B.B.S. and M.S. degrees from Bombay University, Bombay, India, in 1972 and 1976, respectively. He received the MChOrth degree from the University of Liverpool, Liverpool, U.K., in 1979. In December 1994, he received the Ph.D. degree from Twente University, Enschede, The Netherlands, for his thesis on paraplegic locomotion.

He returned to India in 1983 and worked as an orthopaedic surgeon in Nagpur, India. Circumstances brought him back to the United Kingdom in 1985. From December 1985 to May 1993 he worked as a Medical Research Fellow in the Orthotic Research and Locomotor Assessment Unit (ORLAU) at The Robert Jones and Agnes Hunt Orthopaedic and District Hospital in Oswestry, Shropshire, U.K. There he developed his interest in the subjects of human locomotion, paraplegic locomotion, functional electrical stimulation, and cerebral palsy. He was invited to work in the Netherlands. In January 1994, he started work as a Research Fellow in Roessingh Research and Development based at Roessingh Rehabilitation Centre in Enschede, The Netherlands. From July 1994 to June 1997, he retrained as a specialist in Physical and Rehabilitation Medicine. Presently, he works as a specialist in Physical and Rehabilitation Medicine, and continues to work as a Research Fellow in Roessingh Research and Development, based at Roessingh Rehabilitation Centre in Enschede. He has continued his research interests in functional electrical stimulation, gait analysis and its applications in clinical decision making, and balance control in neurological disorders and its relation to walking ability.